ARTICLE

Effects of Oxygen Vacancy on the Adsorption of Formaldehyde on Rutile TiO_2(110) Surface

Li-ming Liu, Jin Zhao*

Hefei National Laboratory for Physical Sciences at Microscale, and Key Laboratory of Strongly-Coupled Quantum Matter Physics, Chinese Academy of Sciences, and Department of Physics, and Synergetic Innovation Center of Quantum Information & Quantum Physics, University of Science and Technology of China, Hefei 230026, China

(Dated: Received on March 22, 2017; Accepted on March 31, 2017)

Oxygen vacancy (O_v) has significant influence on physical and chemical properties of TiO_2 systems, especially on surface catalytic processes. In this work, we investigate the effects of O_v on the adsorption of formaldehyde (HCHO) on TiO_2(110) surfaces through first-principles calculations. With the existence of O_v, we find the spatial distribution of surface excess charge can change the relative stability of various adsorption configurations. In this case, the bidentate adsorption at five-coordinated Ti (Ti_{5c}) can be less stable than the monodentate adsorption. And HCHO adsorbed in O_v becomes the most stable structure. These results are in good agreement with experimental observations, which reconcile the long-standing deviation between the theoretical prediction and experimental results. This work brings insights into how the excess charge affects the molecule adsorption on metal oxide surface.

Key words: TiO_2, Formaldehyde, Oxygen vacancy, Excess electrons

I. INTRODUCTION

Titanium dioxide (TiO_2) is a versatile material for a wide range of applications, to name a few, as UV blocking pigments and sunscreen in industry, mixed conductor and synthetic single crystals semiconductor in electronic devices, most importantly, as abundant and toxic free photocatalyst which have been focused since the water splitting work done by Fujishima and Honda in 1972 [1].

Formaldehyde (HCHO) on TiO_2 is of particular interest because in numerous organic catalytic reactions HCHO is a key species (reactant, intermediate, or product) such as resins synthesis [2], CO_2 reduction [3], and hydrogen production [4]. Besides, HCHO is a common interior pollutant which causes severe health issues, TiO_2-based HCHO decomposing devices play a crucial role in the control of air pollution.

The adsorption of HCHO on TiO_2(110) surface has attracted attentions from both theoretical and experimental researchers for the last two decades [5−9]. Despite numerous innovational materials based on TiO_2 were synthesized to catalyze decomposing HCHO, the theoretical predictions and experimental observation of adsorption configurations of HCHO on TiO_2 were not in accordance, even on the most widely investigated rutile TiO_2 (110) surface. In 2001 for the first time, Idriss *et al.* theoretically addressed the adsorption configurations and energies of HCHO on TiO_2(110) surface using a cluster model based on density functional theory (DFT) calculations [10]. Although only one monodentate adsorption configuration was taken into consideration and the cluster model may not be an accurate description of extended surface, nevertheless, this work pioneered the ambition of using accurate DFT calculations to reveal the micro picture of aldehydes such as HCHO adsorption on metal oxides. In 2011, Haubrich *et al.* reported a systematic investigation of the effects of different surface and subsurface point defects on the adsorption of HCHO on TiO_2(110) surfaces through DFT calculations [11]. They declared a bidentate adsorption configuration which has almost twice the adsorption energy of other monodentate adsorption configurations on five-coordinated Ti (Ti_{5c}). From then on, theoretical studies continued confirming that the bidentate adsorption configuration is the most stable structure. However, the bidentate adsorption configuration was hardly confirmed from experimental observations. For instance, in 2013, Yuan *et al.* reported the photocatalytic oxidation of methanol on TiO_2(110) surface by means of thermal desorption spectroscopy (TPD) and X-ray photoelectron spectroscopy (XPS) [7]. They found the formation of HCHO and the shift of C 1s level indicated that no bidentate configuration was detected. In early 2016, Yu *et al.* reported, at low coverage (submonolayer) and low temperatures (45 K to 65 K), the

*Author to whom correspondence should be addressed. E-mail: zhaojin@ustc.edu.cn

most abundant species of HCHO on TiO_2(110) surface is a chemisorbed monomer bounded to Ti_{5c} sites (Lewis acid) in a tilted monodentate configuration [12]. To understand the deviation between theoretical predictions and experimental observations is urgent.

Recently, the disagreement between the computational and experimental results started decreasing. In 2015, Zhang *et al*. reported that the spatial distribution of the extra charge near a O_v site strongly affected the binding of the Ti-bound formaldehyde, especially decreased the stability of bidentate adsorption configurations [9]. In late 2016, Feng *et al*. reported confirmation of the bidentate configurations of HCHO on Ti_{5c} through STM observations [13].

From the view of experimental endeavor, stoichiometric TiO_2 surfaces are very challenging to grow. They are easily being reduced or reconstructed with various defects and reconstruction. Among various point defects which make TiO_2 a typical *n*-type semiconductor, oxygen vacancy (O_v) is very common. Removing one oxygen atom from the surface would break two Ti−O bonds and release two electrons back to surface, those unpaired electrons are defined as excess charge. It is believed to have significant influence on molecular adsorption and surface catalytic reactions. Therefore, a systematical study on how O_v affect the adsorption of HCHO is essential.

In this work, we reported the adsorption of HCHO on both stoichiometric and reduced TiO_2(110) surfaces. The interaction between molecular adsorption and excess charge was discussed in full details. The relative stability of various adsorption configurations in the presence of excess electrons induced by O_v was investigated through the comparison of geometries, energies and electronic structures. We found that the excess charge induced by O_v affects the adsorption of HCHO significantly. With the existence of O_v, the bidentate adsorption at Ti_{5c}, can be less stable than the monodentate adsorption. And HCHO adsorbed in O_v becomes the most stable structure. These results are in good agreement with experimental observations, which interpret the long-standing deviation between the theoretical prediction and experimental results.

II. CALCULATION METHODS

Periodic DFT calculations were performed by using the vienna *ab initio* simulation package (VASP) [14, 15]. The generalized gradient approximation (GGA) functional was adopted with the Perdew-Burke-Ernzerhof (PBE) exchange-correlation description [16, 17]. The energy cutoff of 400 eV for plane-wave basis sets was used to expand the valence electronic wave function with the configurations of $C(2s^22p^2)$, $H(1s^1)$, $O(2s^22p^4)$ and $Ti(4s^23d^2)$. The projector augmented wave (PAW) method was used to describe the electron-ion interaction. Dipole corrections were adopted to cancel the interactions between the excess charge and its periodic images for all calculations. A 5×2 slab model containing 3 Ti-O-Ti tri-layer was chosen to simulate the TiO_2(110) surfaces. The atoms in the bottom Ti-O-Ti tri-layer were fixed to the positions within bulk TiO_2 during the structure optimization. To screen the effects of un-paired electrons from bottom Ti and O, the pseudo hydrogen saturation method was adopted. Since a Ti atom in TiO_2 bulk offers four electrons to bind to six O atoms and each O atom in bulk bonded to three Ti, pseudo hydrogens with the valence of 2/3 ($H_{0.66}$) and 4/3 ($H_{1.33}$) electron charge were added to bottom O and Ti correspondingly as shown in FIG. 1. The $H_{0.66}$−O and $H_{1.33}$−Ti bond lengths were determined to be 1.02 and 1.88 Å by the geometry optimization procedure which kept all Ti and O atoms fixed in bulk position then allowed the pseudo hydrogen atoms to relax. Then by fixing the bottom layer, the slab was optimized until the force on each atom is smaller than 0.02 eV/Å. To avoid the interlayer interaction, a vacuum layer of 15 Å was added between slabs. To correct the self-interaction error in DFT, we apply U=4.5 eV on Ti 3d orbitals.

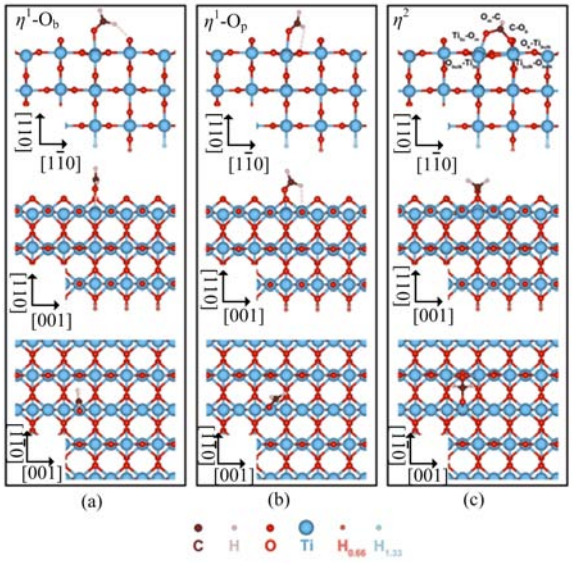

FIG. 1 Adsorption configurations of HCHO on stoichiometric TiO_2(110) surface (η^1-O_b, η^1-O_p and η^2) in side and top views (along [001], [1-10], and [110] directions for upper, middle and lower schemas correspondingly in each box). The axis notations are omitted in the following for simplicity.

The formation energy ($E_{\text{formation}}$) of oxygen vacancy is defined as:

$$E_{\text{formation}} = E_{\text{perfect}} - E_{O_v} - \frac{1}{2}E_{O_2} \qquad (1)$$

E_{perfect} is the total energy of stoichiometric surface, E_{O_v} is the total energy of the same surface with one oxygen vacancy and E_{O_2} is the energy of single oxygen molecule. To compare the stability of various adsorp-

DOI:10.1063/1674-0068/30/cjcp1703049

TABLE I Characteristic bonds (as notated in FIG. 1) and adsorption energies of monodentate and bidentate adsorption configurations at Ti_{5c} on reduced TiO_2(110) surface, total distortion (TD) is the sum of absolute bond-length change of corresponding bonds comparing to same adsorption configuration on stoichiometric surface (η^1_stoi and η^2_stoi).

	$O_{bulk}-Ti_{5c}$/Å	$Ti_{5c}-O_m$/Å	O_m-C/Å	$C-O_b$/Å	O_b-Ti_{bulk}/Å	$Ti_{bulk}-O_{bulk}$/Å		TD/Å	E_{ad}/eV
						Outer	Inner		
η^1_stoi	1.995	2.229	1.232	–	1.884	2.088	2.088	0	−0.83
η^1_offline	1.932	2.274	1.233	–	1.885	2.086	2.087	0.113	−1.24
η^1_online_nn	1.940	2.254	1.231	–	1.886	2.085	2.084	0.090	−1.19
η^1_online_n	1.941	2.252	1.230	–	1.884	2.084	2.086	0.085	−1.17
η^2_stoi	2.169	1.951	1.387	1.419	2.082	1.965	2.056	0	−1.57
η^2_offline	2.240	1.892	1.410	1.432	2.068	1.966	2.052	0.185	−1.99
η^2_online_nn	2.238	1.898	1.394	1.447	2.040	2.009	2.033	0.266	−1.76
η^2_online_n	2.282	1.884	1.410	1.426	2.088	2.007	2.023	0.291	−1.12

tion configurations, we defined the adsorption energy (E_{ad}) as:

$$E_{ad} = E_{TiO_2+HCHO} - E_{TiO_2} - E_{HCHO} \quad (2)$$

where E_{TiO_2+HCHO} is the total energy of HCHO adsorbed on TiO_2(110) surface, E_{HCHO} and E_{TiO_2} are total energies of single HCHO molecule and clean TiO_2(110) surface correspondingly.

III. RESULTS AND DISCUSSION

A. The adsorption of HCHO on stoichiometric TiO_2(110) surface

In agreement with previous reports [9, 11, 13, 18, 19], the calculated most stable adsorption configuration of HCHO on pseudo hydrogen saturated stoichiometric TiO_2(110) surface is the bidentate adsorption configuration (η^2) at Ti_{5c}. FIG. 1 shows the top and side views of two monodentate (η^1) and one bidentate η^2 adsorption structures on Ti_{5c}. For η^2 (FIG. 1(c)), two C−O bonds form sp^3 hybridization other than sp^2 hybridization as HCHO molecule in vacuum or monodentate adsorption configurations (η^1-O_b, η^1-O_p). Since η^1-O_b and η^1-O_p are almost identical either in geometry (FIG. 1 (a) and (b)), adsorption energy or electronic structure [20], the η^1-O_b configuration was chosen as the representative for the two monodentate structures of HCHO at Ti_{5c} and remarked as η^1. The adsorption energy difference between bidentate and monodentate adsorption configurations is 0.7 eV as shown in Table I.

B. Adsorption of HCHO on reduced TiO_2(110) surface with O_v

1. BBO_v as a common defect on TiO_2(110) surface

For TiO_2(110) surface, bridge bonded oxygen vacancy (BBO_v) is known as the most stable O_v structure. It is more stable than in-plane oxygen vacancy (IPO_v) and O_v in sub-surface by 0.36 eV in our calculations. These results are in accordance with previous calculations [21]. Each O_v induces two excess electrons to the system. The two excess electrons prefer occupying sub-surface Ti which is in agreement with previous calculations [22, 23]. For reduced TiO_2(110) surface with BBO_v, there are two sites favorable for HCHO adsorption. One is at surface Ti_{5c}, the other is in BBO_v.

2. HCHO adsorption on Ti_{5c}

For the adsorption of HCHO at Ti_{5c} on reduced TiO_2(110) surface with BBO_v, although adsorption configurations are preserved from those on stoichiometric surface, the adsorption energies and relative stability among these adsorption configurations are significantly affected by the presence of BBO_v.

The first distinguishing feature is that the adsorption energies decrease about 0.4 eV for monodentate adsorption configuration (η^1) on reduced TiO_2(110) surface than on stoichiometric surface. We labeled different Ti_{5c} sites according to their relative position with BBO_v as online_n, online_nn, and offline as shown in FIG. 2. As shown in Table I, for monodentate adsorption configurations, the adsorption energies for η^1_offline, η^1_online_nn, η^1_online_n are −1.24, −1.19, and −1.17 eV. Comparing to −0.83 eV of HCHO on stoichiometric surface in monodentate configurations, molecular adsorption on reduced surface is stabilized. The reason for the energy shift is the electrostatic interaction between excess charge induced by BBO_v and dipole moment from adsorbed HCHO molecules.

Another significant effect is the site sensitivity for bidentate adsorption configuration (η^2) of HCHO on reduced TiO_2(110) surface. It is clearly presented that, for η^2 configurations, the adsorption energy could vary from −1.99 eV to −1.12 eV at different Ti_{5c} sites (FIG. 2(a)−(c)). The adsorption energy dependents on the distance between HCHO and BBO_v. At offline site,

DOI:10.1063/1674-0068/30/cjcp1703049

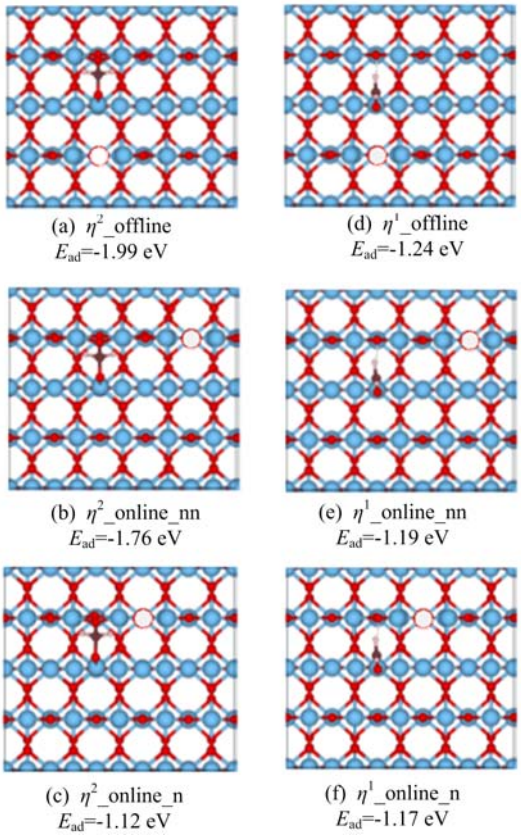

FIG. 2 The top view (along [110] direction) of adsorption configurations of HCHO on TiO_2(110) surface with O_v. Different configurations are labeled as "offline, online_nn and online_n" by the relative distance between the adsorption sites and O_v.

HCHO binds to bridge bonded oxygen which has no O_v in the same row. The local environment is similar to that on stoichiometric surface except there is electrostatic interaction between sub-surface excess electron and adsorbed HCHO molecule. Thus, the adsorption energy decreased from −1.57 eV on stoichiometric surface to −1.99 eV on reduced surface. The 0.4 eV energy shift is similar to the adsorption energies change of monodentate adsorption configuration (η^1) between stoichiometric and reduced surfaces. For HCHO at Ti_{5c} closer to BBO_v (η^2_online_nn and η^2_online_n), lattice distortion becomes larger after the molecular adsorption in Table I. The aggravated distortion would dramatically affect the spatial distribution of excess electrons. The changed distribution of excess electrons alters the electrostatic interaction strength and the adsorption energies for η^2_online_nn and η^2_online_n become −1.76 and −1.12 eV.

The significant site sensitivity of bidentate adsorption configuration is due to the change of the localization of excess charge induced by BBO_v. For η^2_offline, similar to the monodentate adsorption configurations, the excess charge all localized in sub-surface separately as shown in FIG. 4(a)−(d) correspondingly. In this case, the overall electrostatic interaction is attractive leading to stabilize molecular adsorption. For bidentate adsorption structures (η^2_online_nn and η^2_online_n), the aggravated distortion induced by molecular adsorption would drive excess charge to surface localizing closely around BBO_v site then the overall electrostatic interaction is repulsive and the molecular adsorption is destabilized as shown in FIG. 4 (e) and (f).

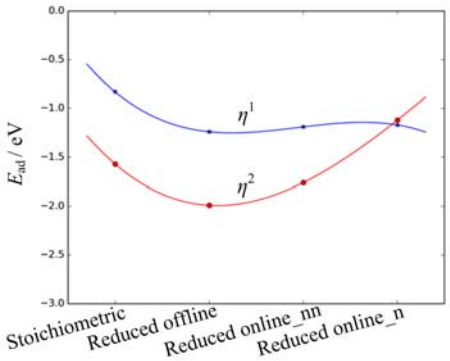

FIG. 3 Comparison of adsorption energy *vs.* adsorption site between monodentate and bidentate adsorption configurations on stoichiometric and reduced TiO_2(110) surfaces.

It should be noticed that the bidentate adsorption configuration, which is the most stable structure on stoichiometric surface, could become the least stable one with the interaction with O_v. Especially when HCHO adsorbing at Ti_{5c} close to BBO_v in FIG. 3, the bidentate adsorption configuration (η^2_online_n) is less stable than all other monodentate adsorption configurations.

3. HCHO adsorption in BBO_v

The adsorption of HCHO in BBO_v heals the vacancy in a manner of inserting oxygen end of HCHO into the vacancy. The symmetric adsorption configuration (sym_η^1-O_v) with molecular oxygen bonded to two five-folded Ti in BBO_v has the adsorption energy of −1.46 eV (FIG. 5 (a)−(c)). Beside this symmetric monodentate adsorption configuration (FIG. 5(a)), another asymmetric monodentate adsorption structure was found with an extra hydrogen bond between molecular H and adjacent bridge oxygen (sym_η^1-O_v). Despite an extra hydrogen bond formed (FIG. 5(b)), the asymmetric adsorption configuration has the adsorption energy of −1.45 eV which is similar to symmetric one because the Ti−O_m bonds are stretched on one side and compressed on the other side. Notice that the adsorption energies of monodentate adsorption configurations at BBO_v are, not only about 0.6 eV lower than monodentate adsorption configurations on stoichiometric surface, but also about 0.2 eV lower than monodentate adsorption configurations at Ti_{5c} with O_v.

DOI:10.1063/1674-0068/30/cjcp1703049

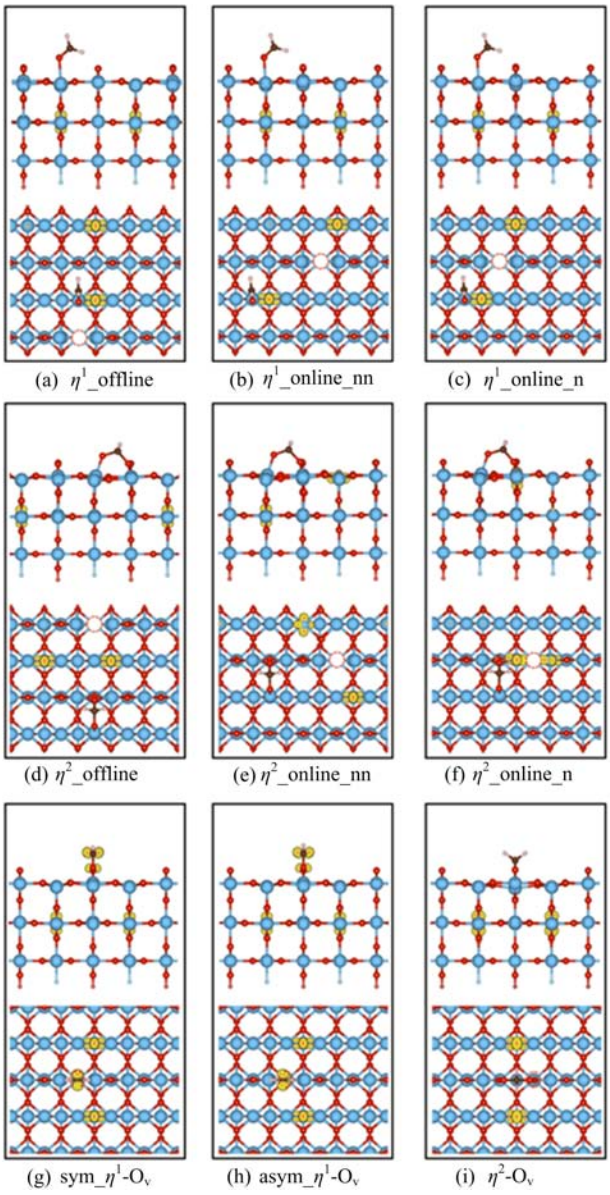

FIG. 4 Distribution of O_v induced excess electrons after adsorption of HCHO on reduced TiO_2(110) in side (along [001] direction) and top (along [110] direction) views. The dashed red circles filled with white represent the position of BBO_v while the empty dashed red circles depict healed BBO_v by HCHO adsorption. Spatial distribution (orbitals) of two excess electrons were depicted in yellow.

A bidentate adsorption configuration (η^2-O_v) can be formed with an extra chemical bond of C−O_b. The adsorption energy of η^2-O_v is −1.70 eV which is the most stable one among all presented adsorption configurations of HCHO close to BBO_v (FIG. 5(c)). In other words, if there are BBO_vs on TiO_2(110) surface, HCHO favors adsorbing at O_v sites rather than Ti_{5c} sites near BBO_v.

The adsorption of HCHO in BBO_v has minor influence on the distribution of excess charge. For sym_η^1-O_v and asym_η^1-O_v, a small amount of excess electron (less than 20%) involved in the Ti−O_m bond formation, the majority of excess electrons (larger than 80%) still locate at sub-surface (FIG. 4 (g) and (h)). For η^2-O_v configuration, another C−O bond forming sp^3 hybridization then no need of excess charge for chemical bonding thus the excess electrons remain localized in sub-surface (FIG. 4(i)).

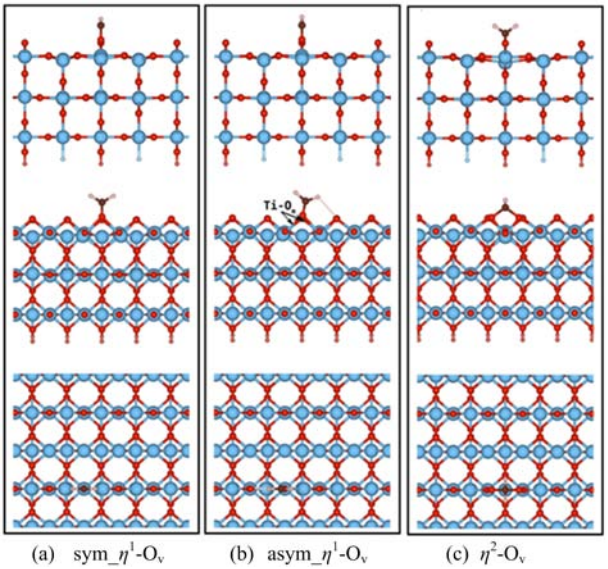

FIG. 5 Adsorption configurations of HCHO in BBO_v on TiO_2(110) surface in side and top views (along [001] [1-10], and [110] directions for upper, middle and lower schemas correspondingly in each box).

4. Effects of HCHO adsorption on the electronic structure

Molecular adsorption affects the electronic structure of reduced TiO_2(110) surface in two ways. On one hand, molecular orbitals could emerge in band gap as HOMO or LUMO of the system; on the other hand, the defect states originated from BBO_v could be affected by molecular adsorption.

For monodentate adsorption configurations at Ti_{5c} (η^1_offline, η^1_online_nn, and η^1_online_n), the highest occupied molecular orbitals are about 0.3 eV bellow the valence band maximum (VBM) of TiO_2 (FIG. 6). The gap states originated from BBO_v are stabilized by molecular adsorption with the downward energy shift of 0.5 eV compared to clear reduced surface. The stabilization of excess charge states is because of the electrostatic attraction between adsorbed HCHO and excess electrons.

For bidentate adsorption configurations at Ti_{5c} (η^2_offline, η^2_online_nn, and η^2_online_n), molecular orbital contributes a gap state about 0.2 eV above VBM. As the adsorption of HCHO approaching to BBO_v (from η^2_offline to η^2_online_nn then

DOI:10.1063/1674-0068/30/cjcp1703049

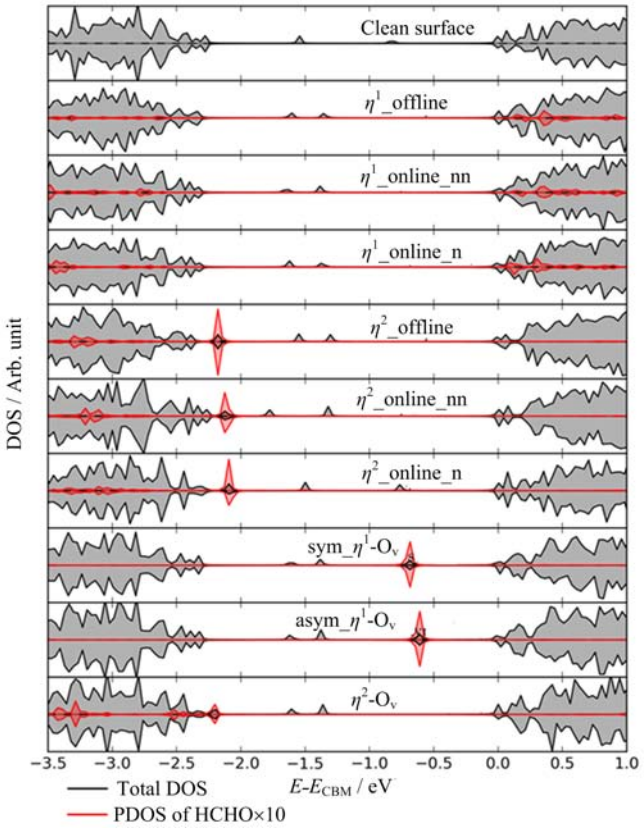

FIG. 6 Density of states (DOS) for various adsorption configurations of HCHO on reduced TiO_2(110) surface. Black line represents total DOS and red line represents the partial DOS of HCHO with the magnification of 10 times for clarity.

η^2_online_n), the molecular gap state shifts upward a little bit due to the larger local structural distortion in Table I. Gap states induced by BBO_v are stabilized for η^2_offline and η^2_online_nn configurations also due to the electrostatic attraction between adsorbed HCHO and excess electrons. For η^2_online_n configuration which is close to BBO_v, these excess charge gap states are destabilized by shifting up about 0.1 eV because the two excess electrons are closely distributed around BBO_v site due to molecular adsorption.

As for HCHO adsorbing in BBO_v in sym_η^1-O_v and asym_η^1-O_v configurations, an empty state from the hybridization of O 2p and Ti 3d emerged about 0.7 eV bellow conduction band minimum (CBM). The excess charge states have about 0.5 eV energy downward shift similar to the monodentate adsorption at Ti_{5c} (η^1_offline, η^1_online_nn, and η^1_online_n). Molecular adsorption is stabilized by excess charge located mainly (larger than 80%) in sub-layer. For HCHO in BBO_v in η^2-O_v configuration, molecular O 2p orbitals contribute a gap state about 0.1 eV above VBM which is similar to HCHO at Ti_{5c} in η^2 configuration. But the excess charge is still located in sub-surface which is similar to HCHO at Ti_{5c} in η^1 configuration.

From above analysis, we argued that the bidentate adsorption configurations of HCHO at Ti_{5c} have great potential to be the hole scavenger, while HCHO in BBO_v in the sym_η^1-O_v and asym_η^1-O_v configurations have the great potential to be the electron scavenger in photocatalytic process on TiO_2(110) surfaces. And molecular adsorption could either stabilize or destabilize the excess charge states by altering the electrostatic interaction between molecular adsorption and BBO_v.

IV. CONCLUSION

In this work, we investigated the adsorption of HCHO on stoichiometric and reduced TiO_2(110) surfaces through first-principles calculations. Compared to stoichiometric surface, oxygen vacancy in reduced TiO_2 would induce excess electrons to the system and affect the relative stability of molecular adsorption configurations. For HCHO adsorbing at Ti_{5c}, on one hand, excess electrons would stabilize molecular adsorption for monodentate adsorption. On the other hand, for bidentate adsorption, the adsorption stability depends strongly on the adsorption site. The adsorption is stabilized when the adsorption is far away from BBO_v. Yet it can be significantly destabilized when the adsorption is close to BBO_v and becomes less stable than the monodentate adsorption. The adsorption in BBO_v is the most stable configuration near BBO_v among all the configurations we investigated. Our calculations reconcile the long-standing discrepancies between theoretical predictions and experimental observations of the HCHO/TiO_2 system and provide valuable insights into the effects of O_v on the molecular adsorption on TiO_2.

V. ACKNOWLEDGMENTS

This work was supported by the National Natural Science Foundation of China (No.21373190, No.21421063, No.11620101003) and the National Key Foundation of China, Department of Science & Technology (No.2016YFA0200600 and No.2016YFA0200604), the Fundamental Research Funds for the Central Universities of China (No.WK3510000005), the support of National Science Foundation (No.CHE-1213189 and No.CHE-1565704). Calculations were performed at Environmental Molecular Sciences Laboratory at the PNNL, a user facility sponsored by the DOE Office of Biological and Environmental Research.

[1] A. Fujishima and K. Honda, Nature **238**, 37 (1972).
[2] Y. H. Lee, C. A. Kim, W. H. Jang, H. J. Choi, and M. S. Jhon, Polymer **42**, 8277 (2001).
[3] B. Kaesler and P. Schönheit, Eur. J. Biochem. **186**, 309 (1989).

DOI:10.1063/1674-0068/30/cjcp1703049

[4] C. Winner and G. Gottschalk, FEMS Microbiol. Lett. **65**, 259 (1989).
[5] G. Busca, J. Lamotte, J. C. Lavalley, and V. Lorenzelli, J. Am. Chem. Soc. **109**, 5197 (1987).
[6] C. B. Xu, W. S. Yang, Q. Guo, D. X. Dai, T. K. Minton, and X. M. Yang, J. Phys. Chem. Lett. **4**, 2668 (2013).
[7] Q. Yuan, Z. F. Wu, Y. K. Jin, L. S. Xu, F. Xiong, Y. S. Ma, and W. X. Huang, J. Am. Chem. Soc. **135**, 5212 (2013).
[8] Q. Yuan, Z. F. Wu, Y. K. Jin, F. Xiong, and W. X. Huang, J. Phys. Chem. C **118**, 20420 (2014).
[9] Z. R. Zhang, M. R. Tang, Z. T. Wang, Z. Ke, Y. B. Xia, K. T. Park, I. Lyubinetsky, Z. Dohnálek, and Q. F. Ge, Top. Catal. **58**, 103 (2015).
[10] L. Kieu, P. Boyd, and H. Idriss, J. Mol. Catal. A-Chem. **176**, 117 (2001).
[11] J. Haubrich, E. Kaxiras, and C. M. Friend, Chemistry **17**, 4496 (2011).
[12] X. J. Yu, Z. R. Zhang, C. W. Yang, F. Bebensee, S. Heissler, A. Nefedov, M. R. Tang, Q. F. Ge, L. Chen, B. D. Kay, Z. Dohnálek, Y. M. Wang, and C. Wöll Christof, J. Phys. Chem. C **120**, 12626 (2016).
[13] H. Feng, L. M. Liu, S. H. Dong, X. F. Cui, J. Zhao, and B. Wang, J. Phys. Chem. C **120**, 24287 (2016).
[14] G. Kresse and J. Hafner, Phys. Rev. B **48**, 13115 (1993).
[15] G. Kresse and J. Furthmuller, Phys. Rev. B **54**, 11169 (1996).
[16] J. P. Perdew, K. Burke, and M. Ernzerhof, Phys. Rev. Lett. **77**, 3865 (1996).
[17] J. P. Perdew, M. Emzerhof, and K. Burke, J. Chem. Phys. **105**, 9982 (1996).
[18] H. Z. Liu, X. Wang, C. X. Pan, and K. M. Liew, J. Phys. Chem. C **116**, 8044 (2012).
[19] M. R. Tang, Z. R. Zhang, and Q. F. Ge, Catal. Today **274**, 103 (2016).
[20] L. M. Liu and J. Zhao, Surf. Sci. **652**, 156 (2016).
[21] M. V. Ganduglia-Pirovano, A. Hofmann, and J. Sauer, Surf. Sci. Rep. **62**, 219 (2007).
[22] P. M. Kowalski, M. F. Camellone, N. N. Nair, B. Meyer, and D. Marx, Phys. Rev. Lett. **105**, 146405 (2010).
[23] T. Shibuya, K. Yasuoka, S. Mirbt, and B. Sanyal, J. Phys. Condens. Matter **24**, 435504 (2012).

DOI:10.1063/1674-0068/30/cjcp1703049